A Phenylalanine Clamp Controls Substrate Specificity in the Quorum-Quenching Metallo-γ-lactonase from Bacillus thuringiensis

8 AUTHORS, INCLUDING:

Dali Liu
Loyola University Chicago
32 PUBLICATIONS **433** CITATIONS

SEE PROFILE

Jessica Momb
University of Texas at Austin
11 PUBLICATIONS **216** CITATIONS

SEE PROFILE

Gregory A. Petsko
Brandeis University
481 PUBLICATIONS **25,259** CITATIONS

SEE PROFILE

Dagmar Ringe
Brandeis University
270 PUBLICATIONS **13,344** CITATIONS

SEE PROFILE

A Phenylalanine Clamp Controls Substrate Specificity in the Quorum-Quenching Metallo-γ-lactonase from *Bacillus thuringiensis*

Ce Feng Liu,[†,⊥] Dali Liu,[‡] Jessica Momb,[∥] Pei W. Thomas,[§] Ashley Lajoie,[†] Gregory A. Petsko,[†] Walter Fast,*[∥,§] and Dagmar Ringe*[†]

[†]Departments of Chemistry and Biochemistry and Rosenstiel Basic Medical Sciences Research Center, Brandeis University, Waltham, Massachusetts 02454, United States

[‡]Department of Chemistry and Biochemistry and Bioinformatics Program, Loyola University Chicago, Chicago, Illinois 60626, United States

[§]Division of Medicinal Chemistry, College of Pharmacy, and [∥]Graduate Program in Biochemistry, The University of Texas, Austin, Texas 78712, United States

ABSTRACT: Autoinducer inactivator A (AiiA) is a metal-dependent *N*-acyl homoserine lactone hydrolase that displays broad substrate specificity but shows a preference for substrates with long *N*-acyl substitutions. Previously, crystal structures of AiiA in complex with the ring-opened product *N*-hexanoyl-L-homoserine revealed binding interactions near the metal center but did not identify a binding pocket for the *N*-acyl chains of longer substrates. Here we report the crystal structure of an AiiA mutant, F107W, determined in the presence and absence of *N*-decanoyl-L-homoserine. F107 is located in a hydrophobic cavity adjacent to the previously identified ligand binding pocket, and the F107W mutation results in the formation of an unexpected interaction with the ring-opened product. Notably, the structure reveals a previously unidentified hydrophobic binding pocket for the substrate's *N*-acyl chain. Two aromatic residues, F64 and F68, form a hydrophobic clamp, centered around the seventh carbon in the product-bound structure's decanoyl chain, making an interaction that would also be available for longer substrates, but not for shorter substrates. Steady-state kinetics using substrates of various lengths with AiiA bearing mutations at the hydrophobic clamp, including insertion of a redox-sensitive cysteine pair, confirms the importance of this hydrophobic feature for substrate preference. Identifying the specificity determinants of AiiA will aid the development of more selective quorum-quenching enzymes as tools and as potential therapeutics.
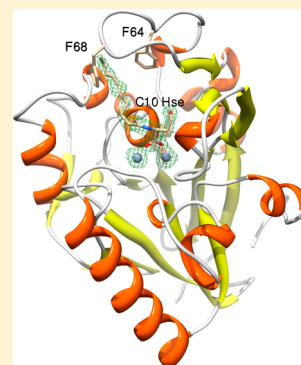
Microbial quorum sensing is a widely employed strategy that bacteria use to coordinate behaviors such as bioluminescence, antibiotic synthesis, biofilm formation, adhesion, swarming, competence, sporulation, virulence, and others.[1] The small molecules that mediate these cell-to-cell communication pathways are numerous and diverse in structure. One large class of signaling molecules consists of *N*-acyl-L-homoserine lactones (AHLs), which share a common (*S*)-α-amino-γ-butyrolactone ring linked by an amide bond to an alkyl substituent with varying lengths, typically consisting of a linear alkane between 4 and 14 carbons long displaying various oxidation states at the 3′ carbon, with the exact substitution pattern depending on the identity of the producing organism.[2] The AHLs are produced by Gram-negative bacteria, usually for intraspecies signaling, although there are examples of interspecies signaling and the related *N*-aroyl-L-homoserine lactones are known to mediate interkingdom signaling.[3−6] The lactone ring of these signals can be nonenzymatically hydrolyzed to yield the ring-opened product *N*-acyl-L-homoserine, which is no longer capable of promoting quorum sensing.[7,8] Ring opening also blocks the nonenzymatic conversion of 3-oxo-AHLs into bacteriocidal tetramic acids.[9] Therefore, the labile lactone moiety presents an attractive target for the use of enzymes to selectively block quorum sensing in

AHL-mediated pathways and to provide antibiotic resistance by blocking the formation of tetramic acids.

Accordingly, the enzyme AiiA (autoinducer inactivator A), which is an AHL hydrolase (also called AHL lactonase, EC 3.1.1.81), was identified in Gram-positive *Bacillus* sp. and was demonstrated to rapidly catalyze the hydrolysis of the AHL ring in a number of different substrates (Figure 1).[10−12] Combined observations from X-ray crystal structures along with steady-state kinetic measurements, alternative metal ion substitutions, substrate analogues, and molecular modeling have led to the proposal of a detailed mechanism in which ring opening is catalyzed through an addition−elimination reaction facilitated by two zinc ions bound together in a dinuclear cluster at the enzyme's active site.[2,12−16] Comparison of unliganded and product-bound structures shows a reorganization of the active site to specifically bind the hydrolyzed lactone moiety. However, only weak, nonspecific interactions were observed between the short *N*-hexanoyl substitution and a wide hydrophobic groove on the surface of the protein.[15,16] Other enzymes in the same metallo-β-lactamase superfamily use
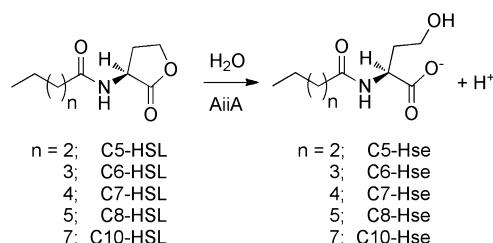
Figure 1. *N*-Acyl-L-homoserine lactonase (AiiA, AHL lactonase) catalyzes the hydrolysis of *N*-acyl-L-homoserine lactones (AHLs, *N*-acyl-HSLs) to yield the corresponding ring-opened products, *N*-acyl-L-homoserines (N-acyl-Hse), which are not recognized as quorum-sensing signals. 3-Oxo-AHLs (not shown) are also accepted as substrates, and their hydrolysis prevents nonenzymatic rearrangement into tetramic acids that have antibiotic properties.

extended β-hairpin loops that act as "flaps" to recruit, stabilize, and properly orient substrates for catalysis, but no associated flap was observed in AiiA.[17] A region close to the active site of AiiA (residues 60−73) was disordered, similar to the highly mobile flaps of other unliganded proteins in this superfamily, suggesting this region as part of a potential flap,[18] but the product's *N*-hexanoyl chain is too short to interact with this site on the protein and instead makes alternative interactions as described above.

Here, we report the discovery of a distal "phenylalanine clamp" composed of F64 and F68 that provides a binding site for AHL substrates with linear *N*-acyl substituents with at least seven carbons. Steady-state kinetics of various length substrates with wild-type and site-directed mutants of AiiA along with X-ray crystal structures of unliganded and *N*-decanoyl-L-homoserine lactone-treated AiiA mutants reveal the importance of this binding site toward catalysis and substrate specificity, leading to a better understanding of how this quorum-quenching protein works and how it might be optimized for various applications.

■ EXPERIMENTAL PROCEDURES

Unless otherwise noted, all chemicals were obtained from Sigma-Aldrich Chemical Co. (St. Louis, MO), and all cloning enzymes were obtained from New England BioLabs (Beverly, MA). The substrates *N*-pentanoyl-(*S*)-homoserine lactone (C5-HSL), *N*-hexanoyl-(*S*)-homoserine lactone (C6-HSL), *N*-heptanoyl-(*S*)-homoserine lactone (C7-HSL), *N*-octanoyl-(*S*)-homoserine lactone (C8-HSL), and *N*-decanoyl-(*S*)-homoserine lactone (C10-HSL) were synthesized according to the procedure reported previously.[12,14,16]

Protein Expression and Purification. *Bacillus thuringiensis* AHL lactonase (AiiA) was expressed and purified as a TEV (tobacco etch virus) protease cleavable fusion to maltose binding protein according to the procedure reported previously unless noted otherwise.[12,19] Briefly, *Escherichia coli* BL21(DE3) cells (Merck, Damstadt, Germany) transformed with the pMAL-t-AiiA vector were grown and induced with 0.5 mM

IPTG. AiiA was purified as described with an additional gel filtration step.[12,19] The concentrated AiiA sample from the final DEAE-Sepharose column step was loaded onto a Hi-Prep 16/60 Sephacryl S-200 HR column (GE Healthcare, Piscataway, NJ) equilibrated in buffer containing 20 mM Tris and 200 mM NaCl (pH 7.4). Fractions containing monomeric AiiA, identified by the elution volume and sodium dodecyl sulfate−polyacrylamide gel electrophoresis, were pooled and concentrated.

Site-Directed Mutagenesis of AiiA. Expression vectors for AiiA F107W and the double mutant F64C/F68C were obtained using the QuikChange II XL site-directed mutagenesis kit from stratagene (La Jolla, CA). Primers used to obtain each mutant are listed in Table 1. Briefly, a QuikChange reaction mixture (50 μL) consisted of 125 ng of forward primer, 125 ng of reverse primer, 100 ng of pMAL-t-AiiA template plasmid,[12] 200 μM dNTPs, and 2.5 units of *Pfu* polymerase in reaction buffer and was subjected to the following thermocycler sequence: 95 °C for 1 min, 18 cycles of 95 °C for 50 s, 60 °C for 50 s, and 68 °C for 7 min, and 68 °C for 7 min. DpnI restriction enzyme was added (10 units) and allowed to digest the parental plasmid in the reaction mixture for 1 h at 37 °C. The DpnI-digested reaction mixture was transformed into competent *E. coli* XL10 Gold Cells (Stratagene) and selected by being plated onto an LB-agar plate supplemented with 100 μg/mL ampicillin. All mutations described herein were verified by fully sequencing the gene inserts (Genewiz, South Plainfield, NJ).

Kinetic Assay of AiiA Activity. The catalytic activity of AiiA was measured spectrophotometrically by the method described previously.[12,19] Protons released from the hydrolysis of AHL substrates in a weakly buffered solution at pH 7.5 were detected with a pH-sensitive dye, phenol red. Briefly, in a typical AiiA activity assay, the decrease in OD$_{557}$ of a 100 μL reaction mixture containing 50 nM enzyme, 75 μM phenol red, and 0−10 mM AHL substrate in 1 mM HEPES and 200 mM NaCl (pH 7.5) was measured over time in a Costar 9017 96-well assay plate (Corning, Corning, NY) using the BioTek PowerWave XS2 microplate spectrophotometer (BioTek, Winooski, VT). Initial reaction rates were calculated on the basis of the initial ΔOD$_{557}$, and a proton standard curve was generated with hydrochloric acid.

Quantification of Free Thiol Groups in the Redox-Sensitive AiiA F64C/F68C Mutant. The number of free thiol groups in variants of AiiA was quantified by a colorimetric assay using Ellman's reagent [5,5′-dithiobis(2-nitrobenzoic acid) (DTNB)].[20] Purified AiiA samples were concentrated to ~250 μM and treated with or without DTT (5 mM) at room temperature for 15 min. Following DTT treatment, excess DTT was removed by passing samples through Zeba microspin desalting columns (Thermo Scientific, Rockford, IL) equilibrated in 100 mM potassium phosphate and 4 M guanidine hydrochloride (pH 8.0). Protein concentrations were redetermined after the desalting column step by the

Table 1. Primers Used for QuikChange Site-Directed Mutagenesis

primer	sequence
F107W forward	5′-GTTCTCACTTACATTGGGATCATGCAGGAGGAAACGG-3′
F107W reverse	5′-CCGTTTCCTCCTGCATGATCCCAATGTAAGTGAGAAC-3′
F64C/F68C forward	5′-CTTTGCAACGGTACATGTGTTGAAGGACAGATC-3′
F64C/F68C reverse	5′-GATCTGTCCTTCAACACATGTACCGTTGCAAAG-3′

Table 2. Steady-State Kinetic Constants of AHL Hydrolysis by AiiA Variants

AiiA variant	substrate	k_{cat} (s^{-1})	K_M (mM)	k_{cat}/K_M (s^{-1} M^{-1})	$(k_{cat}/K_M)_{substrate}/(k_{cat}/K_M)_{C5\text{-}HSL}$ [a]
WT[b]	C5-HSL	43 ± 6	3 ± 1	1.4×10^4	1.0
WT[b]	C6-HSL	36 ± 1	2.1 ± 0.3	1.7×10^4	1.2
WT[b]	C7-HSL	34 ± 2	0.30 ± 0.06	11×10^4	7.9
WT[b]	C8-HSL	34 ± 1	0.18 ± 0.02	19×10^4	14
WT[b]	C10-HSL	54 ± 6	0.14 ± 0.05	39×10^4	28
F107W	C5-HSL	0.08 ± 0.02	6 ± 2	0.0012×10^4	1.0
F107W	C6-HSL	0.257 ± 0.003	10 ± 2	0.0026×10^4	2.2
F107W	C7-HSL	0.30 ± 0.05	1.6 ± 0.5	0.019×10^4	16
F107W	C8-HSL	0.46 ± 0.03	0.8 ± 0.1	0.058×10^4	48
F107W	C10-HSL	0.32 ± 0.07	0.15 ± 0.08	0.21×10^4	180

[a]Ratio of k_{cat}/K_M values for each substrate divided by the reference C5-HSL substrate for each variant of AiiA tested. [b]Wild type.

OD$_{280}$ method and were used directly for the thiol quantification assay. As control experiments, buffer containing either 5 or 0 mM DTT was subjected to the same procedure described above and used as a blank.

The thiol quantification assay was conducted in a 96-well microplate format using the BioTek H1MFG microplate reader. In each reaction mixture, 5 μL of protein sample was added to 95 μL of reaction buffer [100 mM potassium phosphate, 4 M guanidine hydrochloride, and 256 μM DTNB (pH 8.0)]. The formation of a yellow product, 2-nitro-5-thiobenzoic acid (TNB), as a result of DTNB reacting with free thiol groups was measured at 412 nm. OD$_{412}$ measurements were converted to molar concentrations using a standard curve (0−62.5 μM fresh DTT) or directly using the molar extinction coefficient of TNB of 14150 M^{-1} cm^{-1}.[21]

Crystallization. AiiA was crystallized by the hanging drop method using ∼20 mg/mL protein. In a typical hanging drop experiment, 2 μL of AiiA was mixed with 2 μL of well solution [80 mM Tris, 160 mM MgCl$_2$, 24% (w/v) PEG-4000 (pH 8.5), and 20% (w/v) glycerol]. For the cocrystallization of AiiA mutants and C10-HSL, 2 μL of AiiA was mixed with 2 μL of well solution and 0.5 μL of 10 mM C10-HSL (dissolved in 50% methanol). Crystal formation was apparent after incubation at 20 °C for 2−4 days. Crystals with good morphology were cryo-cooled directly in liquid nitrogen.

Crystallographic Data Collection. Data were collected on beamline 23-IDD at GM/CA-CAT of the Advanced Photon Source at Argonne National Laboratory (Argonne, IL). Diffraction data were collected at a wavelength of 1.03 Å, at 100 K on a MarMosaic CCD detector (Rayonix, Evanston, IL), and processed with the HKL2000 software suite.[16]

Structure Determination. AiiA mutant structures with or without ligand bound were determined by molecular replacement using a previously published AHL lactonase structure [Protein Data Bank (PDB) entry 2A7M][13] as an initial search model using PHASER[22] in the CCP4 software suite.[23] Cycles of refinement, including simulated annealing refinement and model rebuilding, were conducted using REFMAC5,[24] PHENIX,[25] and Coot.[26] The coordinates of the ligands were generated using the Dundee PRODRG2 server (http://davapc1.bioch.dundee.ac.uk/programs/prodrg/), and the ligand topology files were generated using the SKETCHER program in the CCP4 program suite. The ligand coordinates were then fit into the difference electron density of the apo AiiA model and included in the next round of refinement along with the topology files.

Figures. All structural figures were made using PYMOL (http://www.pymol.org). The electron density maps were generated with FFT in the CCP4 suite in the CCP4 format.

■ RESULTS

Kinetic Characterization of Dizinc AiiA. To investigate the substrate specificity of dizinc wild-type AiiA, steady-state kinetic constants for five AHL substrates differing only in the length of the aliphatic N-acyl side chain, namely, C5-HSL, C6-HSL, C7-HSL, C8-HSL, and C10-HSL, were determined (Table 2). The k_{cat} values for all substrates were in the range of 34−54 s^{-1}. The K_M values, however, are quite different between substrates with long and short N-acyl substituents. C7-HSL, C8-HSL, and C10-HSL have K_M values approximately 1 order of magnitude lower than those of C5-HSL and C6-HSL. Likewise, as a result of lower K_M values, the overall catalytic efficiencies (k_{cat}/K_M) for C7-HSL, C8-HSL, and C10-HSL are also ∼1 order of magnitude larger than those of C5-HSL and C6-HSL. These k_{cat}/K_M values match those reported earlier for dizinc AiiA and are similar to those reported for AiiA in which the zinc content had not been optimized ($10^3−10^4$ M^{-1} s^{-1}).[11,16] The observed preference for longer substrates is also similar to that observed for the dicobalt form of AiiA.[16]

Kinetic Characterization of Dizinc F107W AHL Lactonase. In an attempt to probe the importance of residues neighboring the active site for substrate binding and catalysis, F107 was mutated to the bulkier hydrophobic residue tryptophan. Compared to the wild-type enzyme, the F107W mutant had impaired enzymatic activity for all AHL substrates tested (Table 2). Catalytic efficiencies (k_{cat}/K_M) decrease by 2−3 orders of magnitude for all AHL substrates, with the greatest impairment observed for the short C5-HSL substrate (approximately 1200-fold decrease). This effect decreases as the length of the substrate's N-acyl substituent increases (approximately 190-fold decrease for the C10-HSL substrate). Relative to that of the wild type, the decreases in k_{cat}/K_M values for the F107W enzyme are largely due to decreases in k_{cat} (≥73-fold) rather than increases in K_M (≤5-fold).

Determination of the Structure of Dizinc F107W AiiA. X-ray crystal structures of dizinc F107W AiiA were determined with and without the addition of substrate C10-HSL. Crystallographic data and refinement statistics are listed in Table 3. The untreated F107W AiiA crystal diffracted to a resolution of 1.72 Å. The substrate-treated F107W AiiA cocrystal diffracted to a resolution of 1.45 Å and was found to contain the ring-opened product, C10-homoserine (C10-Hse) (see below). Structural alignments of unliganded wild-type AiiA (PDB entry 2A7M), unliganded F107W (PDB entry

Table 3. Crystallographic Data and Refinement Statistics

	AiiA F107W	AiiA F107W with C10-Hse
resolution range (Å)	35.2–1.72	45.6–1.45
space group	$P2_12_12_1$	$P2_12_12_1$
cell dimensions		
$\quad a$ (Å)	54.6	54.8
$\quad b$ (Å)	56	55.4
$\quad c$ (Å)	81.3	80.4
total no. of reflections	152763	285247
no. of unique reflections	24982	40145
completeness (%)	92.2 (63.2)[a]	95.9 (68.3)[a]
linear R_{merge} (%)[b]	7 (51)[a]	5.5 (54)[a]
$I/\sigma(I)$	22 (2.1)[a]	29.2 (1.9)[a]
R_{work}, R_{free} (%)[c]	17.9, 21.2	12.0, 15.7
rmsd for bond lengths (Å)	0.016	0.016
rmsd for angle distances (Å)	1.6	1.6
average B (Å^2)	38.3	23.9
Ramachondran plot (%)		
$\quad$ favored	95.6	97.2
$\quad$ allowed	4.4	2.8
PDB entry	4J5F	4J5H

[a]Statistics in parentheses correspond to data in the highest-resolution bin. [b]$R_{merge} = \sum |I_{obs} - I_{avg}|/I_{avg}$. [c]$R_{free} = \sum |F_{obs} - F_{calc}|/F_{calc}$. Five percent of the total reflections were chosen at random as the test set, and only the test set was used to calculate R_{free}. $R_{work} = \sum |F_{obs} - F_{calc}|/F_{calc}$. All reflections except the test set were used to calculate R_{work}.

4J5F), and C10-Hse-bound F107W (PDB entry 4J5H) show that the F107W mutation is accommodated well and does not change the global protein fold (Figure 2).[13] The electron density map of C10-Hse-bound F107W clearly shows the product bound at the active site. Interactions of the product's carboxylate and amide groups with the protein are very similar to those previously observed between the shorter chain C6-Hse product and wild-type AiiA.[15] In both of these product-bound structures, residue D108, which is a zinc-coordinating residue in the apo structure, is located farther from the zinc ion. This

residue was proposed to serve as a proton shuttle during catalysis. In the C10-Hse-bound structure determined here, the oxygen atom of the D108 carboxylate is now 3.7 Å from the zinc ion, beyond the typical bond length for a coordination bond. However, two clear differences between the C6-Hse and C10-Hse product-bound structures are observed. First, the orientation of the alcohol group of the longer C10-HSe product is changed from hydrogen bonding with the catalytic D108 in wild-type AiiA to now making a hydrogen bond (2.9 Å N–O distance) with the indole nitrogen of the mutant F107W side chain (Figure 2). Second, positioning of the longer N-acyl substituent of C10-Hse diverges from that of the shorter product C6-Hse by a 144° rotation around the carbon 1–carbon 2 bond; it is instead held in a previously unrecognized binding pocket (Figure 3). The distal end of the 10-carbon N-acyl substituent is clamped in place by the hydrophobic side chains of F64 and of F68, which are both situated on a surface loop (residues 58–73) that has higher B values than the core of the protein. Carbons 5–10 of the N-acyl substituent of C10-Hse are within van der Waals interaction distance (5 Å) of the F64–F68 pair, which is centered around carbon 7 of the N-acyl substituent.

Kinetic Characterization of F64C/F68C AiiA. To probe the contribution of the phenylalanine clamp (residues F64 and F68) to the preference of AiiA for longer AHL substrates, the F64C/F68C double mutant was prepared. Steady-state kinetics were determined for this double mutant in the presence and absence of 2 mM DTT using C5-HSL and C8-HSL as representative short and long substrates, respectively (Table 4). The C8-HSL substrate was chosen because it was of sufficient length to interact with the phenylalanine clamp and because longer substrates might use nonspecific hydrophobic interactions with residues past the clamp to partially overcome any negative effects of the mutation. In the absence of DTT, the enzymatic activity of F64C/F68C AiiA is impaired as compared to that of the wild-type enzyme, and this reduction is more severe for the long C8-HSL substrate than for the short C5-HSL substrate. The k_{cat} value is decreased by 14- and 41-fold
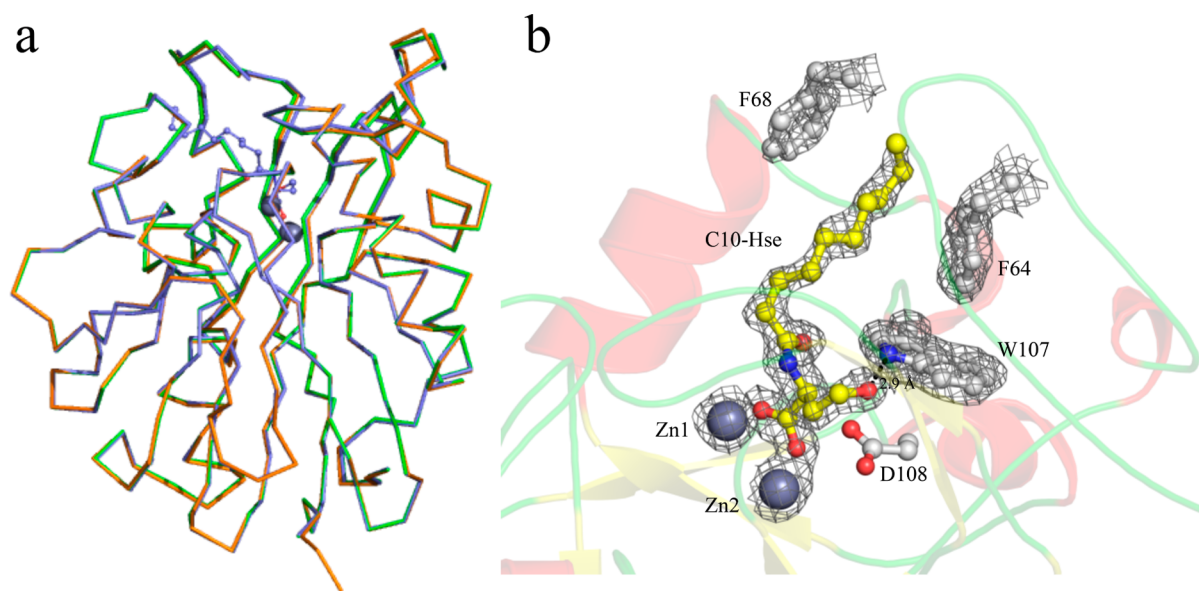

Figure 2. (a) Structural overlay of wild-type AiiA (PDB entry 2A7M, green), unliganded F107W AiiA (PDB entry 4J5F, orange), and C10-Hse-bound F107W AiiA (PDB entry 4J5H, blue). (b) Active site of C10-Hse-bound F107W AiiA. The electron density map ($2F_o - F_c$) at 1σ is colored gray. Carbon atoms of the C10-Hse product ligand are colored yellow.
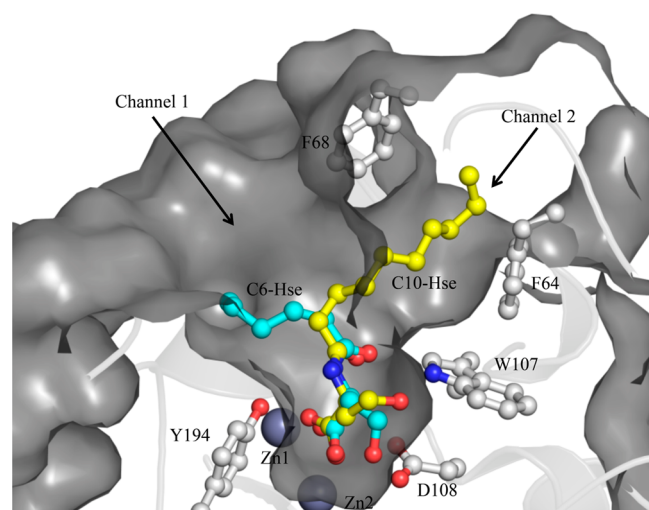
Figure 3. Structural overlay of C6-Hse-bound AiiA and C10-Hse-bound F107W AiiA. Carbon atoms in the C6-Hse product are colored cyan and carbon atoms in the C10-Hse product yellow. The surface representation of AiiA is colored gray and is shown with a cut-away view to reveal interior residues.

and the K_M by 2- and 4-fold, resulting in 21- and 158-fold decreases in k_{cat}/K_M for the C5-HSL and C8-HSL substrates, respectively. The preference for C8-HSL over C5-HSL, as calculated by their k_{cat}/K_M ratios, is now only 1.8-fold, decreased from the 14-fold preference of the wild-type enzyme. However, when DTT is added, enzymatic activity is partially restored. Relative to wild-type AiiA in the presence of DTT (Table 4), the decrease in k_{cat}/K_M values for F64C/F68C AiiA is now ≤2.4-fold. The addition of DTT not only partially restores enzyme activity but also recovers the characteristic substrate specificity of the wild-type enzyme. In the presence of DTT, the F64C/F68C AiiA mutant is now 9.1-fold more specific for C8-HSL than C5-HSL, which is similar to the 11-fold preference of wild-type AiiA [in the presence of DTT (Table 4)].

According to the sequence information and previously determined crystal structure,[13] wild-type AiiA possesses four cysteine residues and no disulfide bonds. The F64C/F68C variant should possess two extra cysteine residues that are close to each other in space as well as in primary sequence. To monitor the formation of a disulfide bond between the two introduced cysteine residues, we determined the number of free thiol groups in the purified AiiA protein samples. As purified without DTT treatment, the number of free cysteines in the AiiA F64C/F68C variant is very similar to the number in the wild-type AiiA protein, approximately 4 equiv (Figure 4). After
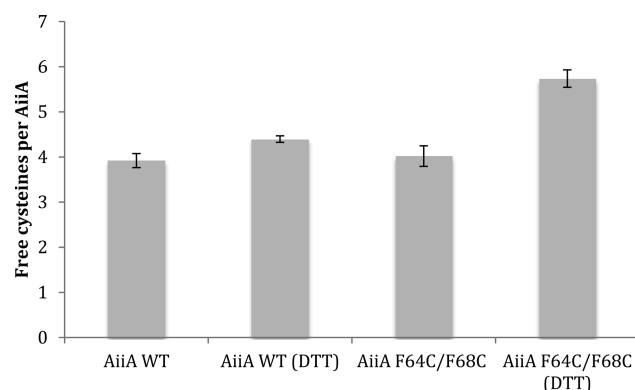

Figure 4. Quantification of free thiol groups in wild-type and F64C/F68C AiiA, before and after treatment with DTT. The average value of three parallel measurements for each protein sample is shown with the standard deviation.

DTT treatment, the number of free cysteines in the AiiA F64C/F68C variant increases significantly to 6 equiv. This increase is consistent with the conclusion that the newly introduced C64 and C68 residues in the mutant AiiA form a disulfide bond that can be reduced by treatment with DTT.

■ DISCUSSION

The growing field of sociomicrobiology focuses on microbial cell-to-cell communication.[27] These intercellular communication pathways are important for diverse phenomena, including the processes that define the composition of mixed microbial cultures, biofilm formation, antibiotic resistance mechanisms, virulence factor production, and others.[1] The development of chemical and biochemical tools for precisely modulating these quorum-sensing pathways has made possible our improved understanding of the molecular basis of the apparent multicellular behaviors in these single-cell organisms.[28] One commonly used diagnostic tool for AHL-based quorum sensing is the enzyme AiiA, a broad specificity AHL lactonase that catalyzes the hydrolysis of N-acyl-HSL substrates to their corresponding N-acyl-Hse products, thereby blocking (or "quenching") quorum sensing.[29,30] Our laboratories and others have elucidated much of the catalytic mechanism that AiiA uses to recognize and hydrolyze the lactone moiety of AHLs.[2,10−16,18,31,32] However, there is only a limited understanding of how the N-acyl substituent of these substrates is recognized. All of the known AHL signals have the same lactone moiety but vary in the identity of their N-acyl substituents. So, obtaining a better understanding of how AiiA recognizes this part of the substrate is essential for developing more precise tools for blocking AHL signals of

Table 4. Steady-State Kinetic Constants of Hydrolysis of AHL by Wild-Type and F64C/F68C AiiA in the Presence or Absence of DTT

AiiA variant	DTT	substrate	k_{cat} (s^{-1})	K_M (mM)	k_{cat}/K_M (s^{-1} M^{-1})	$(k_{cat}/K_M)_{substrate}/(k_{cat}/K_M)_{C5-HSL}$ [a]
F64C/F68C	no	C5-HSL	3.0 ± 0.2	4.5 ± 0.7	0.067 × 10^4	1.0
F64C/F68C	no	C8-HSL	0.83 ± 0.08	0.7 ± 0.2	0.12 × 10^4	1.8
F64C/F68C	yes	C5-HSL	6.1 ± 0.3	1.8 ± 0.3	0.34 × 10^4	1.0
F64C/F68C	yes	C8-HSL	8.2 ± 0.2	0.26 ± 0.03	3.2 × 10^4	9.4
WT[b]	yes	C5-HSL	45 ± 4	6 ± 1	0.75 × 10^4	1.0
WT[b]	yes	C8-HSL	57 ± 7	0.7 ± 0.2	8.1 × 10^4	11

[a]Ratio of k_{cat}/K_M values for each substrate divided by the reference C5-HSL substrate for each variant of AiiA tested under the described experimental conditions. [b]Wild type.

particular lengths, for developing effective quorum-quenching protein therapeutics, and for deepening our basic understanding of how this class of enzyme recognizes and discriminates between substrates.[28,30]

Previously, we reported X-ray crystal structures of AiiA bound to the product C6-Hse.[15] Two different orientations of the product were observed, one of which was still ligated through its newly formed carboxylate to the active-site metal ion cluster. However, the N-hexanoyl chain appeared to make only weak interactions along the surface of a wide groove (marked Channel 1 in Figure 3), and this weak interaction was corroborated by the high mobility of this moiety observed in molecular modeling studies and by the limited impact (≤3.6-fold change in k_{cat}/K_M) of introducing disruptive mutations into this site.[16] Therefore, to improve our understanding of the binding determinants for the N-acyl chain of AHL substrates, we used a combination of approaches, including X-ray crystallography, site-directed mutagenesis, and steady-state kinetics.

As a baseline, we first determined the steady-state rate constants of dizinc AiiA for hydrolysis of AHL substrates with N-acyl substituents of various lengths. The k_{cat}/K_M values increased with increasing substrate length, with substrates bearing N-acyl substituents having at least seven carbons displaying values approximately 1 order of magnitude higher than the shorter substrates (Table 2). This trend was also observed in earlier reports for dicobalt AiiA and for AiiA in which the metal content had not been optimized.[11,16]

In an attempt to probe the importance of selected residues, an F107W mutation was created to perturb substrate binding by introducing additional steric bulk next into the active site. This change had a large negative impact on the activity of the enzyme and produced k_{cat}/K_M values 3 orders of magnitude lower. The decrease was driven mostly by decreased k_{cat} values, so we initially suspected that the proximity of the F107W mutation to the catalytic D108 residue perturbed the positioning of the reaction's proton-shuttling residue. The F107W mutation also has a secondary effect of increasing the specificity of AiiA for longer chain AHLs, with C10-HSL now showing a 180-fold preference over C5-HSL, but this increase in specificity comes at the expense of lower turnover rates.

To improve our understanding of this preference for longer substrates and the lower turnover rates, we crystallized F107W in the absence and presence of C10-HSL. The structure of F107W AiiA determined in the absence of C10-HSL revealed a structure of the unliganded enzyme that was nearly superimposeable with that of wild-type AiiA, with no changes to the overall fold of the protein.[13] Comparison of the active sites also showed negligible changes in the positioning of the zinc ions or the catalytic D108, contrary to our initial expectations. Only a slight side chain rotation at position 107 is sufficient to accommodate the increased bulk of the Trp residue. The structure of F107W AiiA determined in the presence of C10-HSL was more informative. The ring-opened product C10-Hse was observed in the structure, bound to the active-site zinc ion cluster, indicating that the crystal structure likely represents the active form of the enzyme. The positioning of the product's carboxylate and amide moieties is nearly identical to that observed for C6-Hse and wild-type AiiA, but the rest of the product's conformation shows two notable differences.[15] First, the product's primary alcohol (which originated as the lactone's leaving group) was previously found to hydrogen bond with the active-site proton shuttle, D108. However, now it instead

makes a hydrogen bond (2.9 Å N−O distance) with the indole side chain introduced by the F107W mutation. This new interaction might result in tighter product binding and subsequently lower turnover rates. However, K_M values for the substrate and K_i values for the product are on a similar order of magnitude for wild-type enzyme, resulting in negligible product inhibition of initial rates.[14] The carboxylate of D108 in this mutant likely retains its function as the proton shuttle, as it was proposed for the wild-type enzyme.[15] Second, the most obvious change is a repositioning of the N-acyl substituent into a previously unidentified binding pocket. Rotation around the C1−C2 bond of the N-acyl chain repositions the rest of the decanoyl group into a hydrophobic environment on the protein (marked Channel 2 in Figure 3). This alternative binding pocket is lined by residues V69, I73, F107W, and, most prominently, a pair of residues, F64 and F68, that form a phenylalanine clamp around the substrate's N-acyl chain. In contrast to Channel 1, Channel 2 is much smaller and closes down around the substrate. The F68 side chain is disordered in unliganded AiiA, and the entire loop comprising residues 60−73 is disordered in an inhibitor-bound AiiA structure.[13,18] Here, the same region is now ordered but has slightly higher B values than the core of the protein, suggesting that F68 may work as a part of a flexible flap that folds over the substrate. Although the identity and placement of this loop differ from those of other enzymes in the same superfamily, the strategy of using an aromatic residue perched at the apex of a flexible loop to recruit and bind substrates appears to be conserved.[17] With the active-site zinc ion cluster chelated to the product's carboxylate, the enzyme's phenylalanine clamp (F64 and F68) can close down on the other side of the substrate, with the clamp centered around carbon 7 of the N-acyl substituent. This observation is consistent with the steady-state kinetics of both wild-type and F107W AiiA described above in which substrates with at least seven carbons in their linear N-acyl substituents have k_{cat}/K_M values 1 order of magnitude higher than those of shorter substrates that would not be long enough to interact with this phenylalanine clamp.

To understand the structurally implicated phenylalanine clamp in substrate binding and catalysis, its function was tested directly by replacement with a F64C/F68C double mutation. In their reduced forms, the cysteine residues were predicted to provide less hydrophobic surface than the phenylalanine residues to support specific substrate binding. In their oxidized state, a disulfide bond between these two cysteine residues would provide a steric block to inhibit productive substrate binding even more drastically. A similar experimental approach has previously been taken by introducing redox-sensitive cysteine pairs into a voltage-gated sodium ion channel.[33] Introduction of the F64C/F68C double mutation does result in an enzyme whose activity is dependent on the oxidation state of the cysteines. As isolated, the enzyme contains two fewer free thiol groups than predicted, consistent with formation of a disulfide bond between the mutated sites (Figure 4). This variant protein is less active than wild-type AiiA, although the decrease in k_{cat}/K_M values is not as severe as that observed with the F107W mutation. This result is consistent with the location of the phenylalanine clamp being somewhat removed from the catalytic dizinc metal center. More notably, the F64C/F68C double mutation, most likely found in its disulfide-linked form, removes the preference of the enzyme for longer substrates; C8-HSL is now only 1.8-fold favored over C5-HSL (Table 4). The same assays were repeated in the presence of DTT to

reduce the putative F64C/F68C disulfide bond and thereby remove this steric block (Figure 4). As predicted, DTT treatment restores enzyme activity as well as the preference of the enzyme for longer substrates, with C8-HSL now favored 9.4-fold over C5-HSL, as compared to a similar 11-fold preference shown by wild-type AiiA (under the same experimental conditions) (Table 4). These results are consistent with the proposed role of F64 and F68 serving as a hydrophobic phenylalanine clamp that contributes to enforcing the substrate specificity of AiiA.

CONCLUSION

Structural and functional analyses of two AiiA variants have identified a previously unrecognized substrate binding phenylalanine clamp (F64 and F68) and elucidated how this clamp contributes to substrate binding and turnover. The phenylalanine clamp facilitates hydrolysis of AHL substrates with linear N-acyl substituents with at least seven carbon atoms by binding the N-acyl substituent and assisting the substrate to achieve a productive conformation, possibly by sliding the N-acyl chain through the clamp until the lactone engages the catalytic residues and the dinuclear zinc ion cluster responsible for catalyzing the ring-opening reaction. We note that with our identification of an alternative N-acyl binding site, AiiA now has two known hydrophobic sites capable of binding alkyl substituents. Related proteins such as alkylsulfatase SdsA1 and phospholipase D are known to process lipids, so the discovery of two alkyl binding sites on AiiA raises the question of whether this enzyme or an ancestor originally evolved to process two-chain substrates such as diacylphospholipids.[34,35] Regardless of its historical development, AiiA is one of the most efficient and useful quorum-quenching enzymes for blocking AHL signaling. The elucidation of the basis for its substrate preference provides essential information for developing AiiA variants with tailored selectivity as biochemical tools and as potential treatments for plant and animal infections that rely on AHL signaling.

AUTHOR INFORMATION

Corresponding Author

*D.R.: Departments of Chemistry and Biochemistry and Rosenstiel Basic Medical Sciences Research Center, Brandeis University, Waltham, MA 02454-9110; telephone, (781) 736-4902; fax, (781) 736-2405; e-mail, ringe@brandeis.edu. W.F.: Division of Medicinal Chemistry, College of Pharmacy, The University of Texas, Austin, TX 78712; e-mail, waltfast@mail.utexas.edu.

Present Address

[⊥]Department of Neurology and Neuroscience, Weill Cornell Medical College, New York, NY 10065.

ACKNOWLEDGMENTS

REFERENCES

(1) Waters, C. M., and Bassler, B. L. (2005) Quorum sensing: Cell-to-cell communication in bacteria. *Annu. Rev. Cell Dev. Biol. 21*, 319−346.

(2) Fast, W., and Tipton, P. A. (2011) The enzymes of bacterial census and censorship. *Trends Biochem. Sci. 37*, 7−14.

(3) Galloway, W. R., Hodgkinson, J. T., Bowden, S. D., Welch, M., and Spring, D. R. (2011) Quorum sensing in Gram-negative bacteria: Small-molecule modulation of AHL and AI-2 quorum sensing pathways. *Chem. Rev. 111*, 28−67.

(4) Soares, J. A., and Ahmer, B. M. (2011) Detection of acyl-homoserine lactones by *Escherichia* and *Salmonella*. *Curr. Opin. Microbiol. 14*, 188−193.

(5) Schaefer, A. L., Greenberg, E. P., Oliver, C. M., Oda, Y., Huang, J. J., Bittan-Banin, G., Peres, C. M., Schmidt, S., Juhaszova, K., Sufrin, J. R., and Harwood, C. S. (2008) A new class of homoserine lactone quorum-sensing signals. *Nature 454*, 595−599.

(6) Momb, J., Yoon, D. W., and Fast, W. (2010) Enzymic disruption of N-aroyl-L-homoserine lactone-based quorum sensing. *ChemBioChem 11*, 1535−1537.

(7) Horswill, A. R., Stoodley, P., Stewart, P. S., and Parsek, M. R. (2007) The effect of the chemical, biological, and physical environment on quorum sensing in structured microbial communities. *Anal. Bioanal. Chem. 387*, 371−380.

(8) Decho, A. W., Frey, R. L., and Ferry, J. L. (2011) Chemical challenges to bacterial AHL signaling in the environment. *Chem. Rev. 111*, 86−99.

(9) Kaufmann, G. F., Sartorio, R., Lee, S. H., Rogers, C. J., Meijler, M. M., Moss, J. A., Clapham, B., Brogan, A. P., Dickerson, T. J., and Janda, K. D. (2005) Revisiting quorum sensing: Discovery of additional chemical and biological functions for 3-oxo-N-acylhomoserine lactones. *Proc. Natl. Acad. Sci. U.S.A. 102*, 309−314.

(10) Dong, Y. H., Xu, J. L., Li, X. Z., and Zhang, L. H. (2000) AiiA, an enzyme that inactivates the acylhomoserine lactone quorum-sensing signal and attenuates the virulence of *Erwinia carotovora*. *Proc. Natl. Acad. Sci. U.S.A. 97*, 3526−3531.

(11) Wang, L. H., Weng, L. X., Dong, Y. H., and Zhang, L. H. (2004) Specificity and enzyme kinetics of the quorum-quenching N-acyl homoserine lactone lactonase (AHL-lactonase). *J. Biol. Chem. 279*, 13645−13651.

(12) Thomas, P. W., Stone, E. M., Costello, A. L., Tierney, D. L., and Fast, W. (2005) The Quorum-Quenching Lactonase from *Bacillus thuringiensis* Is a Metalloprotein. *Biochemistry 44*, 7559−7569.

(13) Liu, D., Lepore, B. W., Petsko, G. A., Thomas, P. W., Stone, E. M., Fast, W., and Ringe, D. (2005) Three-dimensional structure of the quorum-quenching N-acyl homoserine lactone hydrolase from *Bacillus thuringiensis*. *Proc. Natl. Acad. Sci. U.S.A. 102*, 11882−11887.

(14) Momb, J., Thomas, P. W., Breece, R. M., Tierney, D. L., and Fast, W. (2006) The quorum-quenching metallo-γ-lactonase from *Bacillus thuringiensis* exhibits a leaving group thio effect. *Biochemistry 45*, 13385−13393.

(15) Liu, D., Momb, J., Thomas, P. W., Moulin, A., Petsko, G. A., Fast, W., and Ringe, D. (2008) Mechanism of the quorum-quenching lactonase (AiiA) from *Bacillus thuringiensis*. 1. Product-bound structures. *Biochemistry 47*, 7706−7714.

(16) Momb, J., Wang, C., Liu, D., Thomas, P. W., Petsko, G. A., Guo, H., Ringe, D., and Fast, W. (2008) Mechanism of the quorum-quenching lactonase (AiiA) from *Bacillus thuringiensis*. 2. Substrate modeling and active site mutations. *Biochemistry 47*, 7715−7725.

(17) Huntley, J. J., Fast, W., Benkovic, S. J., Wright, P. E., and Dyson, H. J. (2003) Role of a solvent-exposed tryptophan in the recognition and binding of antibiotic substrates for a metallo-β-lactamase. *Protein Sci. 12*, 1368−1375.

(18) Kim, M. H., Choi, W. C., Kang, H. O., Lee, J. S., Kang, B. S., Kim, K. J., Derewenda, Z. S., Oh, T. K., Lee, C. H., and Lee, J. K. (2005) The molecular structure and catalytic mechanism of a quorum-quenching N-acyl-L-homoserine lactone hydrolase. *Proc. Natl. Acad. Sci. U.S.A. 102*, 17606−17611.

(19) Thomas, P. W., and Fast, W. (2011) Heterologous over-expression, purification, and in vitro characterization of AHL lactonases. *Methods Mol. Biol. 692*, 275−290.

(20) Ellman, G. L. (1959) Tissue sulfhydryl groups. *Arch. Biochem. Biophys. 82*, 70−77.

(21) Eyer, P., Worek, F., Kiderlen, D., Sinko, G., Stuglin, A., Simeon-Rudolf, V., and Reiner, E. (2003) Molar absorption coefficients for the reduced Ellman reagent: Reassessment. *Anal. Biochem. 312*, 224−227.

(22) McCoy, A. J., Grosse-Kunstleve, R. W., Adams, P. D., Winn, M. D., Storoni, L. C., and Read, R. J. (2007) Phaser crystallographic software. *J. Appl. Crystallogr. 40*, 658−674.

(23) Collaborative Computational Project, Number 4 (1994) The CCP4 suite: Programs for protein crystallography. *Acta Crystallogr. D5*, 760−763.

(24) Murshudov, G. N., Vagin, A. A., and Dodson, E. J. (1997) Refinement of macromolecular structures by the maximum-likelihood method. *Acta Crystallogr. D53*, 240−255.

(25) Adams, P. D., Afonine, P. V., Bunkoczi, G., Chen, V. B., Davis, I. W., Echols, N., Headd, J. J., Hung, L. W., Kapral, G. J., Grosse-Kunstleve, R. W., McCoy, A. J., Moriarty, N. W., Oeffner, R., Read, R. J., Richardson, D. C., Richardson, J. S., Terwilliger, T. C., and Zwart, P. H. (2010) PHENIX: A comprehensive Python-based system for macromolecular structure solution. *Acta Crystallogr. D66*, 213−221.

(26) Emsley, P., and Cowtan, K. (2004) Coot: Model-building tools for molecular graphics. *Acta Crystallogr. D60*, 2126−2132.

(27) Parsek, M. R., and Greenberg, E. P. (2005) Sociomicrobiology: The connections between quorum sensing and biofilms. *Trends Microbiol. 13*, 27−33.

(28) Lowery, C. A., Salzameda, N. T., Sawada, D., Kaufmann, G. F., and Janda, K. D. (2010) Medicinal chemistry as a conduit for the modulation of quorum sensing. *J. Med. Chem. 53*, 7467−7489.

(29) Dong, Y. H., Wang, L. H., and Zhang, L. H. (2007) Quorum-quenching microbial infections: Mechanisms and implications. *Philos. Trans. R. Soc. B 362*, 1201−1211.

(30) Amara, N., Krom, B. P., Kaufmann, G. F., and Meijler, M. M. (2011) Macromolecular inhibition of quorum sensing: Enzymes, antibodies, and beyond. *Chem. Rev. 111*, 195−208.

(31) Liao, R. Z., Yu, J. G., and Himo, F. (2009) Reaction mechanism of the dinuclear zinc enzyme N-acyl-L-homoserine lactone hydrolase: A quantum chemical study. *Inorg. Chem. 48*, 1442−1448.

(32) Liu, D., Thomas, P. W., Momb, J., Hoang, Q. Q., Petsko, G. A., Ringe, D., and Fast, W. (2007) Structure and specificity of a quorum-quenching lactonase (AiiB) from *Agrobacterium tumefaciens*. *Biochemistry 46*, 11789−11799.

(33) Benitah, J. P., Tomaselli, G. F., and Marban, E. (1996) Adjacent pore-lining residues within sodium channels identified by paired cysteine mutagenesis. *Proc. Natl. Acad. Sci. U.S.A. 93*, 7392−7396.

(34) Hagelueken, G., Adams, T. M., Wiehlmann, L., Widow, U., Kolmar, H., Tummler, B., Heinz, D. W., and Schubert, W. D. (2006) The crystal structure of SdsA1, an alkylsulfatase from *Pseudomonas aeruginosa*, defines a third class of sulfatases. *Proc. Natl. Acad. Sci. U.S.A. 103*, 7631−7636.

(35) Wang, J., Okamoto, Y., Morishita, J., Tsuboi, K., Miyatake, A., and Ueda, N. (2006) Functional analysis of the purified anandamide-generating phospholipase D as a member of the metallo-β-lactamase family. *J. Biol. Chem. 281*, 12325−12335.